Glycyrrhizic-Acid-Based Carbon Dots with High Antiviral Activity by Multisite Inhibition Mechanisms

Ting Tong, Hongwei Hu, Junwei Zhou, Shuangfei Deng, Xiaotong Zhang, Wantao Tang, Liurong Fang, Shaobo Xiao,* and Jiangong Liang*

With the gradual usage of carbon dots (CDs) in the area of antiviral research, attempts have been stepped up to develop new antiviral CDs with high biocompatibility and antiviral effects. In this study, a kind of highly biocompatible CDs (Gly-CDs) is synthesized from active ingredient (glycyrrhizic acid) of Chinese herbal medicine by a hydrothermal method. Using the porcine reproductive and respiratory syndrome virus (PRRSV) as a model, it is found that the Gly-CDs inhibit PRRSV proliferation by up to 5 orders of viral titers. Detailed investigations reveal that Gly-CDs can inhibit PRRSV invasion and replication, stimulate antiviral innate immune responses, and inhibit the accumulation of intracellular reactive oxygen species (ROS) caused by PRRSV infection. Proteomics analysis demonstrates that Gly-CDs can stimulate cells to regulate the expression of some host restriction factors, including DDX53 and NOS3, which are directly related to PRRSV proliferation. Moreover, it is found that Gly-CDs also remarkably suppress the propagation of other viruses, such as pseudorabies virus (PRV) and porcine epidemic diarrhea virus (PEDV), suggesting the broad antiviral activity of Gly-CDs. The integrated results demonstrate that Gly-CDs possess extraordinary antiviral activity with multisite inhibition mechanisms, providing a promising candidate for alternative therapy for PRRSV infection.

1. Introduction

Carbon dots (CDs), a carbon-based zero-dimensional material also known as carbon quantum dots, are a carbon nanomaterial and a kind of spherical carbon particles with a size below 10 nm.[1] Due to their unique properties in photoluminescence, water solubility, biocompatibility, and resistance to photobleaching as well as cost-effective synthesis and low toxicity, CDs have been extensively investigated,[2–4] and are widely utilized in bio-imaging, bio-sensing, bio-labeling, photodynamic therapy, and drug delivery.[5,6] CDs have a small size and controllable surface functional groups, which facilitate their high adsorption interactions with different biological surfaces.[7] Recently, functionalized CDs synthesized by hydrothermal method have been shown to have antiviral activity.[8–14] However, the antiviral mechanism of these CDs remains to be further elucidated, and the response of cells to them is still unknown.

The most important ingredients of traditional Chinese medicines are Chinese herbal medicines, herbs and plant preparations, which are used worldwide for their anti-oxidation, anti-inflammatory, antiviral immune regulation, antitumor, and other pharmacological functions.[15] Under the conditions of high cost of antiviral drugs and limited healthcare resources, Chinese herbs have been recommended to prevent and treat respiratory disease and herpes simplex in China, especially in poor regions.[16,17] To date, no critically appraised evidence is available on the beneficial effect of Chinese herbal medicines on H1N1 influenza, mainly due to lack of both repeated test of intervention and placebo-controlled trial.[18,19] Furthermore, Chinese herbal poisoning incidents have also been reported.[20,21]

As a common Chinese herbal medicine and a major component of glycyrrhiza uralensis, glycyrrhizic acid has been characterized with various biological activities, such as antiviral immunoregulation, anti-oxidation, anti-inflammation, and liver protection.[22–26] Owing to the ability to inhibit multidrug-resistance-associated proteins, glycyrrhetate and glycyrrhizic acid are used in clinic for cisplatin resistance reversal in hepatocellular carcinoma cells and reduction in liver damage.[27–30] However, glycyrrhizic acid also has the disadvantages of poor water solubility and certain cytotoxicity.[31]

Porcine reproductive and respiratory syndrome (PRRS) is a disease that has been seriously jeopardizing the development of the worldwide pig industry for over two decades.[32] PRRS virus (PRRSV), an enveloped single positive-strand RNA virus, is the

Dr. T. Tong, H. Hu, S. Deng, X. Zhang, W. Tang, Prof. J. Liang
College of Resource and Environment
College of Science
State Key Laboratory of Agricultural Microbiology
Huazhong Agricultural University
Wuhan 430070, P. R. China
E-mail: liangjg@mail.hzau.edu.cn
J. Zhou, Prof. L. Fang, Prof. S. Xiao
State Key Laboratory of Agricultural Microbiology
College of Veterinary Medicine
Key Laboratory of Preventive Veterinary Medicine in Hubei Province
The Cooperative Innovation Center for Sustainable Pig Production
Huazhong Agricultural University
Wuhan 430070, P. R. China
E-mail: vet@mail.hzau.edu.cn

etiologic agent of the disease.[33] To date, PRRSV has no effective treatment in the clinic, and the current authorized prevention and treatment strategy involving the use of inactivated and attenuated vaccine cannot block the occurrence and spread of the disease.[34] Previous studies have investigated many microbicides as potential anti-PRRSV agents to eliminate PRRSV in the body at any stage of PRRSV presence. These microbicides include protein,[35] microRNAs,[36,37] antisense oligonucleotides,[38–41] chemical compounds,[30,42] and nanobodies.[43] They are shown to inhibit virus adsorption, invasion, replication, release, and cell-to-cell spread by restricting cell tropism and targeting the PRRSV genome. However, they have a relatively slight anti-PRRSV effect, with a maximal inhibitory effect of ≈3 orders of magnitude.[32,36–41,43–47]

In this study, a kind of highly biocompatible Gly-CDs was synthesized from active ingredient of Chinese herbal medicine, which combines the high biocompatibility of CDs with the excellent antiviral properties of glycyrrhizic acid and inhibit the proliferation of PRRSV by ≈5 orders of magnitude.

2. Results

2.1. Characterization of CDs

The size and surface morphology of the Gly-CDs were characterized by high-resolution transmission electron microscopy (HR-TEM). As shown by the HR-TEM image in **Figure 1**a, Gly-CDs were round shaped and well-dispersed with a uniform size distribution. Figure 1b showed the size distribution of Gly-CDs measured with a dynamic light scattering (DLS) analyzer. Consistent with the TEM image, Gly-CDs showed high monodispersity, with a calculated average size of 11.4 nm. As shown by the X-ray diffraction (XRD) pattern in Figure 1c, Gly-CDs possessed the component of amorphous carbon due to the broad peak at around 20°.[48] The sharp peak at around 14.9° may be ascribed to the crystallinity of Gly-CDs, and the graphitic carbon accounted for only a small amount of Gly-CDs carbon, so no apparent lattice fringe could be observed in the TEM image.[49] The above results provide evidence that the Gly-CDs are polymeric CDs.

The UV–vis absorption and fluorescence (FL) spectra of the Gly-CDs are presented in Figure 1d. The tiny absorption peak at 260 nm was attributed to $\pi–\pi^*$ transition. The Gly-CDs possessed a significant characteristic blue fluorescence at 438 nm, with the maximal excitation wavelength remaining at 356 nm. Meanwhile, excitation-dependent fluorescence emission was observed when Gly-CDs were excited with different wavelengths from 300 to 410 nm(Figure 1e), due to the normal size distribution of Gly-CDs.[50] The UV–vis absorption spectrum and fluorescence spectrum are all consistent with CDs reported before.[49,51] Figure 1f shows the Gly-CDs functional groups measured by the Fourier transform infrared spectroscopy (FT-IR). In the spectra of Gly-CDs, five obvious absorption peaks could be observed at 3430, 2947, 1621, 1408, and 1051 cm^{-1}, corresponding, respectively, to O−H, C−H, C = C, C = O, and C−O, indicating that Gly-CDs are rich in −OH and −COOH on the surface.[52] The results obtained from the preliminary analysis of the FT-IR spectrum proved that the Gly-CDs conserved

part functional groups of glycyrrhizic acid. The elemental constituents and functional groups of Gly-CDs were further characterized by X-ray photoelectron spectroscopy (XPS). Figure 1g shows the full-scan spectrum of Gly-CDs. The two peaks of C 1s and O 1s could be obviously recognized at 285 and 532 eV, respectively. The elemental analysis demonstrated that Gly-CDs contained 78.25% of carbon and 21.48% of oxygen. The high resolution XPS spectra of the C1s in Gly-CDs could be resolved into three peaks (Figure 1h). The peak at 284.5 eV was assigned to C = O of the carboxylic groups, while the other two peaks at 286.5 and 288.2 eV were ascribed, respectively, to C−O and C−C/C = C.[53,54]

The citric-acid-based CDs (Cit-CDs) were used to act as the contrast, because citric acid and ethylenediamine, the raw materials, do not show antiviral activity. We prepared biocompatible Cit-CDs using the method described in the Supporting Information.[50] As can be seen from TEM and DLS images, the average size of the Cit-CDs was 6.0 nm (Figure S1, Supporting Information). As shown in Figure S2, Supporting Information, a characteristic absorption peak could be observed at 340 nm by UV–vis absorption spectrum, the maximum emission of the Cit-CDs was centered at 455 nm whereas the maximum excitation was recorded at 349 nm in the FL excitation and emission spectra. The results of the FT-IR spectrum suggested that the Cit-CDs were rich in −COOH and −NH$_2$ on the surface while the ^{1}H NMR spectrum indicating the Cit-CDs are highly carbonized. Figure S3, Supporting Information displays the full scan XPS spectrum of Cit-CDs, and elemental analysis indicated that the Cit-CDs consisted of 67.81% of carbon, 13.63% of nitrogen, and 18.56% of oxygen.

2.2. Dose- and Time-Dependent Cytotoxicity of Gly-CDs and Glycyrrhizic Acid on MARC-145 Cells

To assess the biocompatibility of Gly-CDs with the raw materials glycyrrhizic acid in vitro, cytotoxicity experiments were performed. Briefly, MARC-145 cells were cultured separately with glycyrrhizic acid or Gly-CDs at different concentrations for 12, 24, 36, and 48 h. The test results are shown in **Figure 2**. Notably, the viability was more than 80% for MARC-145 cells when treated with Gly-CDs at 0.90 mg mL^{-1} (Figure 2a), in contrast to the viability of ≈60% when treated with glycyrrhizic acid at 0.45 mg mL^{-1} (Figure 2b), which are similar to the cytotoxic concentrations reported in other literature.[55,56] The morphology of the cells treated with the CDs and glycyrrhizic acid for 36 h is shown in Figure S4, Supporting Information. These experimental results indicated that the biocompatibility of Gly-CDs was significantly improved when compared with glycyrrhizic acid. Finally, the 0.30 mg mL^{-1} concentration was selected for further assays. Cytotoxicity assay results for Cit-CDs on MARC-145 cells are depicted Figure S5, Supporting Information.

2.3. Gly-CDs Exhibit Antiviral Activity on PRRSV

The anti-PRRSV activity of glycyrrhizic acid has been reported previously.[30] CDs have good biocompatibility, but its antiviral
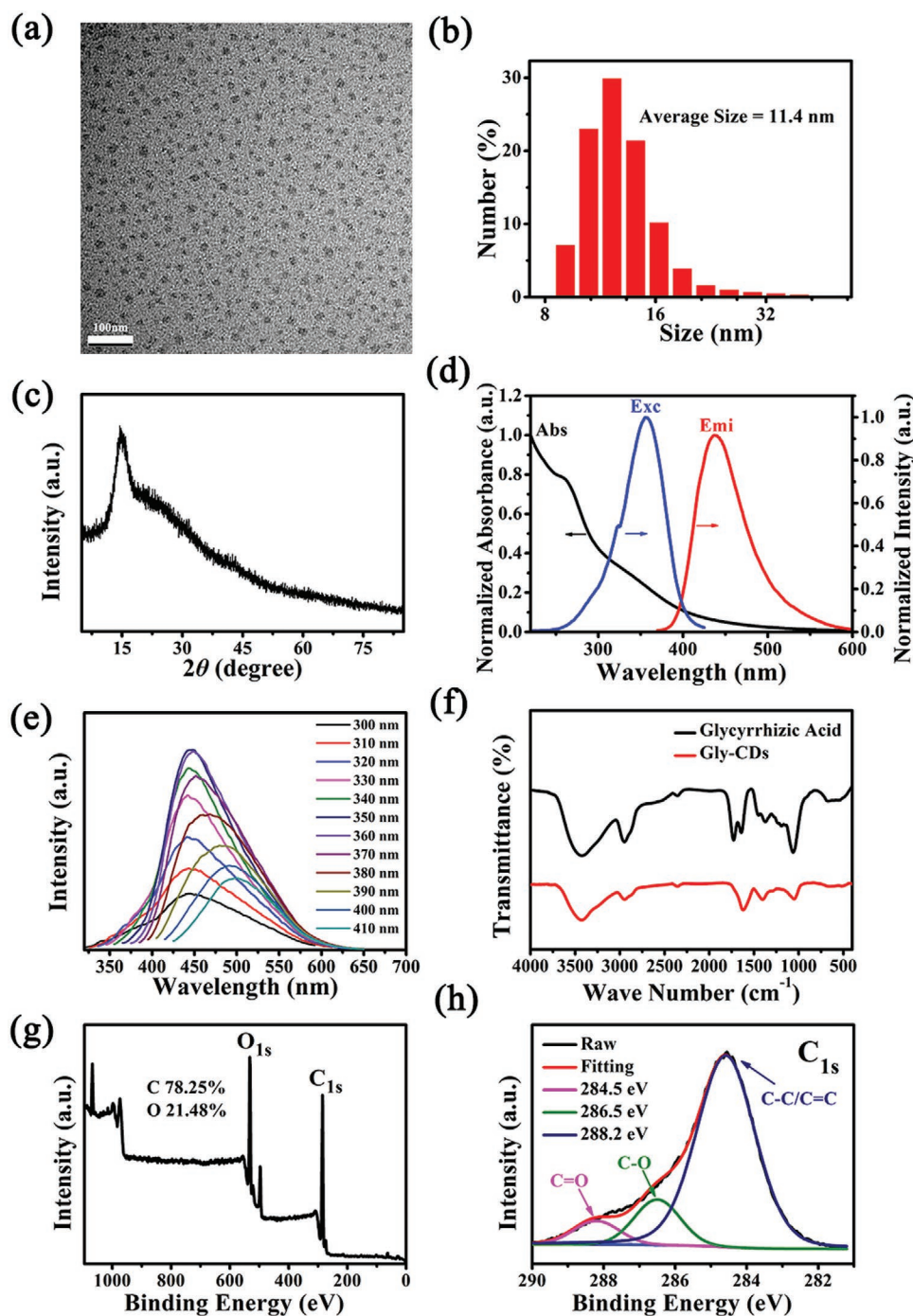
Figure 1. a) TEM image of the Gly-CDs (scale bar = 100 nm); b) DLS analysis of the Gly-CDs; c) XRD pattern of the Gly-CDs; d) UV–vis absorption (black), fluorescence excitation (blue), and emission (red) spectra of the Gly-CDs; e) FL spectra of the Gly-CDs excited with different wavelengths; f) FT-IR spectra of the glycyrrhizic acid and the Gly-CDs. g) Full scans XPS spectrum and h) high-resolution C 1s XPS spectrum of the Gly-CDs.

effect is specific. Here, we focused on the antiviral activity of Gly-CDs and also explored the effects of traditional Cit-CDs on PRRSV proliferation. Plaque assay was used to detect virus infectivity and count the number of viral particles, with the results being expressed in titers. According to the experimental design (Scheme S1, Supporting Information), the addition of Gly-CDs significantly reduced PRRSV titers in intracellular

and cell supernatants at 12, 24, 36, and 48 h post infection (hpi), with a maximal reduction of $\approx 10^5$-fold by plaque assay (**Figure 3**a,b), demonstrating the strong antiviral effect of Gly-CDs on PRRSV. Meanwhile, Cit-CDs showed no inhibitory effect on the proliferation of PRRSV.

The influence of Gly-CDs on PRRSV proliferation was further investigated by analyzing the expression levels of
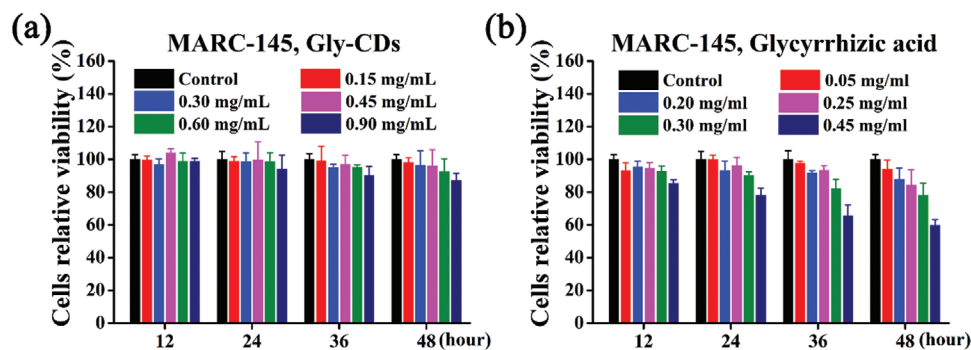
Figure 2. Cytotoxicity of the Gly-CDs and glycyrrhizia acid on MARC-145 cells. a) MARC-145 cells were cultured separately with different concentrations of Gly-CDs (0–0.90 mg mL^{-1}) for 12, 24, 36, and 48 h. b) MARC-145 cells were cultured separately with different concentrations of glycyrrhizic acid (0–0.45 mg mL^{-1}) for 12, 24, 36, and 48 h. Error bars represent the standard deviation from three repeated experiments.
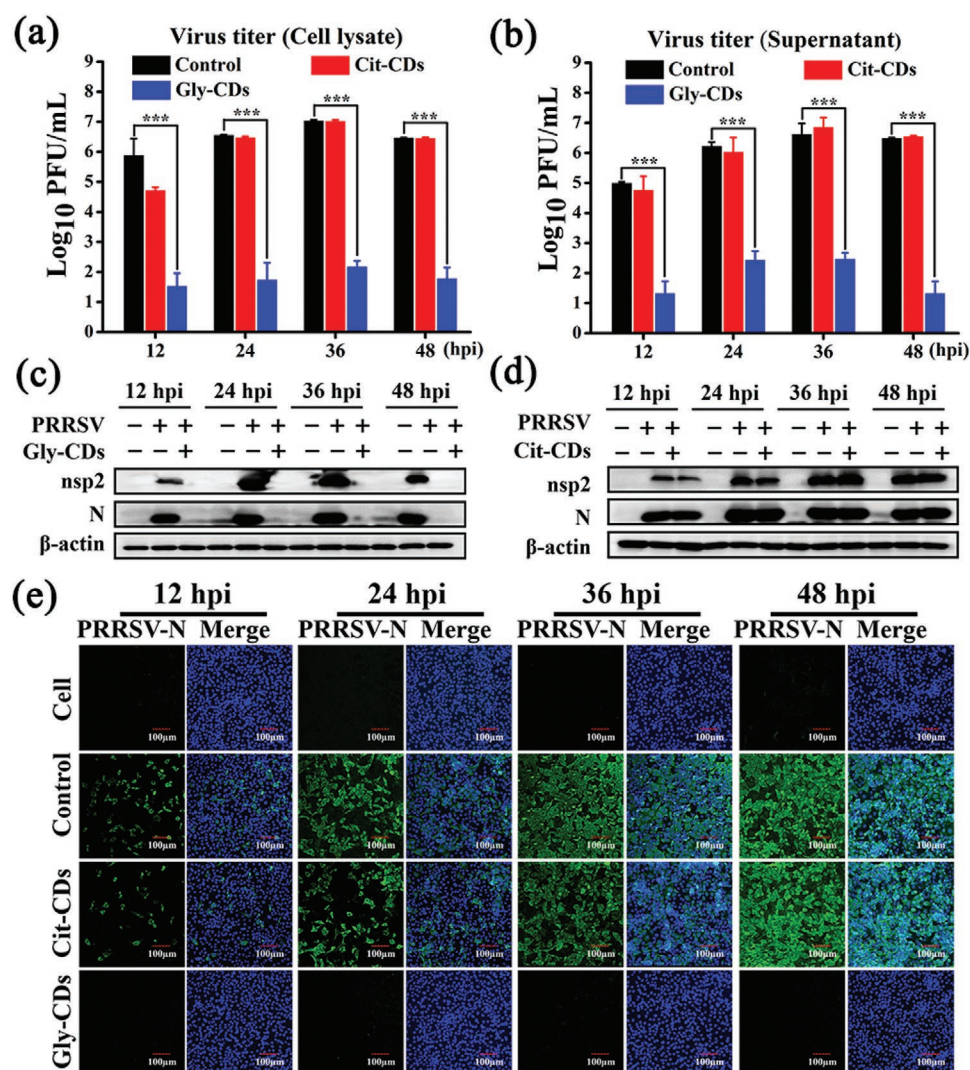
Figure 3. Antiviral activity of Gly-CDs on PRRSV. Growth curves of a) intracellular and b) supernatant PRRSV treated with Gly-CDs and Cit-CDs detected by plaque assay, the mean value was calculated by the t test (mean ± SD, $n = 3$). *$p < 0.05$, **$p < 0.01$, ***$p < 0.001$, compared with the indicated group. Western blot analysis of the expression levels of PRRSV c) nsp2 and d) N proteins under the treatment of Gly-CDs and Cit-CDs at the concentration of 0.30 mg mL^{-1}. e) The IFA images of PRRSV-infected MARC-145 cells treated and untreated with 0.30 mg mL^{-1} Gly-CDs and Cit-CDs at 12, 24, 36, and 48 hpi, respectively. Blue represents the nucleus and green represents the N protein of PRRSV, the field of view is random. Scale bar = 100 μm.

ADVANCED
SCIENCE NEWS
www.advancedsciencenews.com

NANO · MICRO
small
www.small-journal.com

the PRRSV nucleocapsid (N) protein, one structural protein encoded by PRRSV open reading frame 7 (ORF7) gene as the viral capsid protein, and the nonstructural protein 2 (nsp2), a protein with a critical role in viral replication.[34] Western blot assay also revealed a remarkable decrease in the expression levels of PRRSV N and nsp2 proteins under the treatment of Gly-CDs (Figure 3c,d). Meanwhile, indirect immunofluorescence assay (IFA) failed to detect the fluorescence images of PRRSV N proteins at all tested time points (12, 24, 36, and 48 hpi) under the treatment of Gly-CDs (Figure 3e). Nuclei are indicated by the blue fluorescence signal counterstained with 2-(4-amidinophenyl)-6-indolecarbamidine dihydrochloride (DAPI), and the green fluorescence signal represents PRRSV N protein contents stained with a mouse mAb specific for PRRSV N protein and Alexa Fluor 488-conjugated donkey anti-mouse IgG. In the above experiments, MARC-145 cells were infected with PRRSV (multiplicity of infection, MOI = 1) for the indicated periods of time. All these observations indicate Gly-CDs can significantly inhibit PRRSV multiplication.
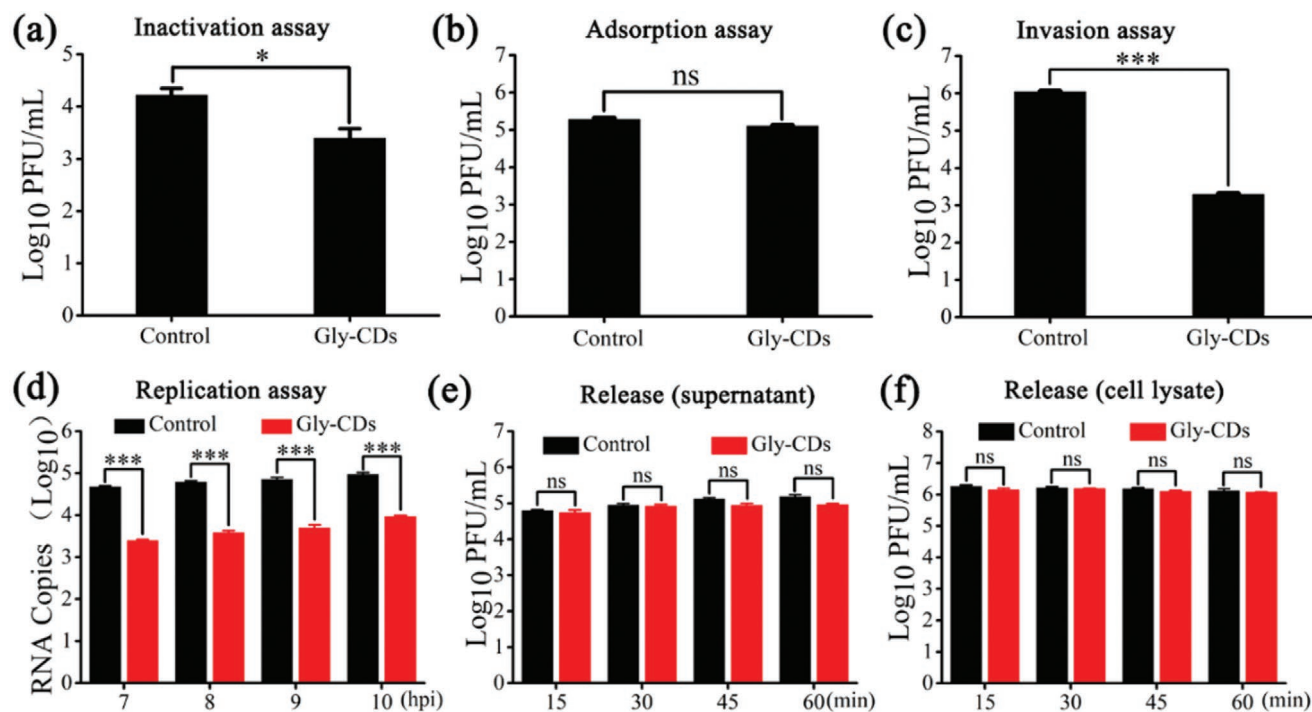
2.4. Gly-CDs Inhibit PRRSV Invasion and Replication

The potential mechanism for the antiviral properties of Gly-CDs were explored by analyzing their effects on the PRRSV proliferation at each stage (adsorption, invasion, replication, and release). Whether Gly-CDs can directly inactivate PRRSV was first tested. As shown in **Figure 4**a, Gly-CDs reduced the number of PRRSV by ≈10-fold by plaque assay, indicating that Gly-CDs can directly inactivate PRRSV. In the adsorption

process of PRRSV, the plaque assay showed no significant difference in the experimental group and control group about their suppression effect on PRRSV adsorption (Figure 4b). In the invasion process of PRRSV, the experimental data revealed that the Gly-CDs treatment decreased the infectious virus titer by about 10^3-fold relative to the control group (Figure 4c), implying that Gly-CDs may suppress PRRSV mainly through inhibiting PRRSV invasion. The influence of Gly-CDs on viral replication was evaluated by real-time quantitative reverse transcription PCR (RT-qPCR) analysis of the negative-sense RNA level of PRRSV. As shown in Figure 4d, Gly-CDs reduced the number of PRRSV RNA copies by nearly 10-fold, revealing their slight influence on PRRSV at the replication stage. Moreover, the effect of Gly-CDs on the release of progeny PRRSV was examined. In Figure 4e,f, no noticeable difference was observed in the virus titers of both intracellular and supernatant PRRSV between the experimental group and control group, suggesting that Gly-CDs had no inhibitory effect on the release of progeny PRRSV. Taken together, Gly-CDs suppress PRRSV proliferation by targeting the invasion and replication processes, with a certain direct inactivation effect in vitro as indicated by statistical analysis, but without any inhibitory effect on the adsorption and release of progeny virus.

2.5. Gly-CDs Inhibit the Proliferation of Coronavirus and Herpesviridae

The antiviral effect of Gly-CDs on the other viruses was further explored by using pseudorabies virus (PRV) and porcine

Figure 4. Multiple-stage inhibition of Gly-CDs on PRRSV proliferation. a) The effect of Gly-CDs on direct inactivation of PRRSV. The effect of Gly-CDs to the infectivity of MARC-145 cells on the b) adsorption, c) invasion, d) replication, and e,f) release processes of PRRSV. The mean value was calculated by the t test (mean ± SD, $n = 3$). *$p < 0.05$, **$p < 0.01$, ***$p < 0.001$, ns, non-significant difference, compared with the indicated group.

epidemic diarrhea virus (PEDV), two causal agents for catastrophic economic losses in the pig industry, as a representative of herpes virus and coronavirus, respectively. The PRV is an enveloped, double-stranded DNA virus in the family Herpesviridae,[57] while PEDV is a large-enveloped RNA virus in the genus, alphacoronavirus of the coronavirus family.[58] In this study, the cytotoxicities of Gly-CDs on Vero cells and PK-15 cells were evaluated first. As shown in **Figure 5**a,c, the viability of either cell line was more than 70% when treated with Gly-CDs at 0.90 mg mL^{-1} for 12 and 24 h. Then, the effects of Gly-CDs on the proliferation of PEDV and PRV were detected by IFA. In Figure 5b, the blue fluorescence signal stained with DAPI represents nuclei, and the green fluorescence signal represents PEDV N protein stained with mouse mAb specific for PEDV N protein and Alexa Fluor 488-conjugated donkey anti-mouse IgG. In Figure 5d, the recombinant PRV expressing green fluorescent protein (PRV-GFP) was transfected into PK-15 cells. The number of PEDV- or PRV-infected cells were shown to be obviously reduced by Gly-CDs versus the control group. These results suggested that Gly-CDs have significant antiviral activity on different viruses, including RNA and DNA viruses.

2.6. Gly-CDs Stimulate Interferon Production in MARC-145 Cells

Interferons (IFN), the major components of natural immunity, play a critical role in antiviral activity. PRRSV can interfere with both the induction of host interferons and the function of antiviral interferon-stimulating genes (ISGs).[59] Whether Gly-CDs promote the production of interferons was explored by RT-qPCR analysis of the mRNA expression levels of ISGs after incubating MARC-145 cells with or without Gly-CDs at 0.30 mg mL^{-1} in DMEM (containing 2% FBS) for 24 h. Meanwhile, in the positive control group, MARC-145 cells were incubated with the Sendai virus (SEV) for 12 h to stimulate the host's natural immunity to produce a large amount of type 1 interferon. The group without Gly-CDs treatment was used as a negative control. As shown in **Figure 6**, compared with the negative control, Gly-CDs treatment showed an obvious increase in the mRNA expression levels of interferon-stimulated genes, ISG-54, ISG-56, ISG-60, oligoadenylate synthetase (OAS), and zinc finger antiviral protein (ZAP). To date, ISG-54, ISG-56, ISG-60, OAS, and ZAP are the ISGs which have been considered to positively regulate the expression of phosphorylated signal transducer and activator of transcription
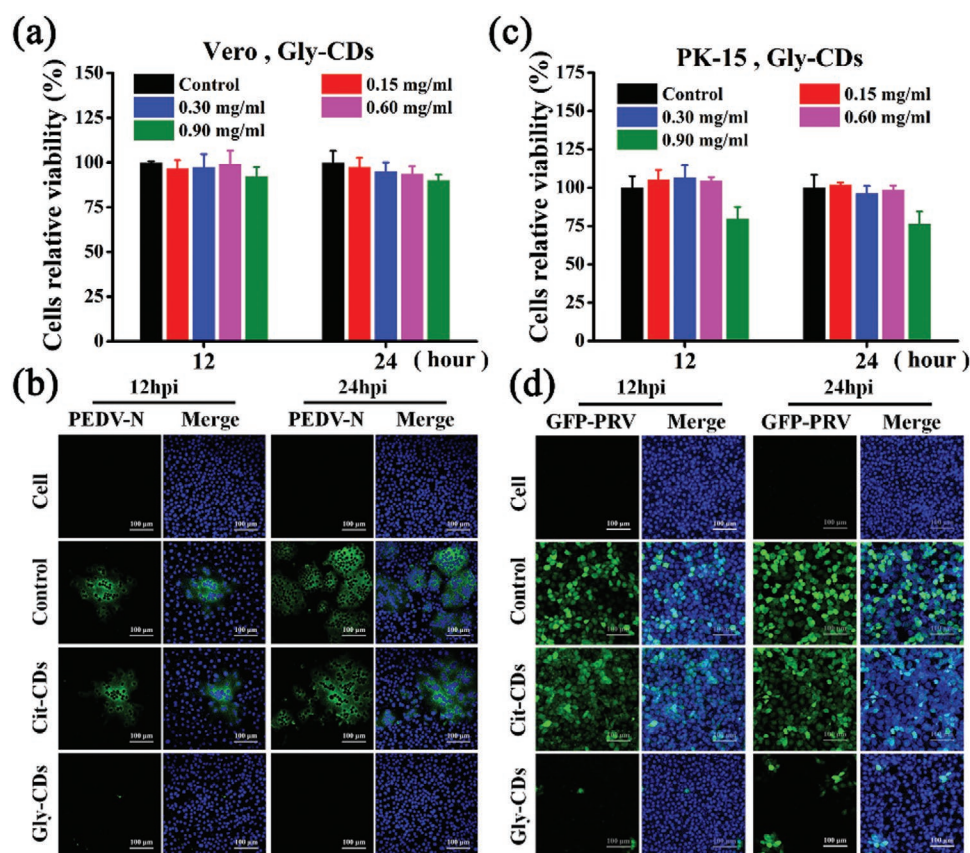
Figure 5. The broad-spectrum antiviral activity of Gly-CDs. a,c) Vero and PK-15 cells were incubated separately with Gly-CDs at the concentrations of 0.15, 0.30, 0.60, and 0.90 mg mL^{-1} for 12 and 24 h. Error bars represent the standard deviation from three repeated experiments. b,d) The IFA images of PEDV-infected Vero cells or PRV-infected PK-15 cell in the absence and presence of 0.30 mg mL^{-1} Gly-CDs at 12 and 24 hpi, respectively. The blue fluorescence signal stained with DAPI represents nuclei, the green fluorescence signal represents PEDV N protein stained with mouse mAb specific for PEDV N protein and Alexa Fluor 488-conjugated donkey anti-mouse IgG. For the above experiments, PK-15 cells were infected with GFP-PRV (MOI = 1) for the indicated periods of time. Vero cells were infected with PEDV (MOI = 0.1) for the indicated periods of time. Scale bar = 100 μm.

1/IFN-β/retinoic acid-inducible gene-G to inhibit viral infection and exert various antiviral and pro-inflammatory reactions.[60–66] These results imply that Gly-CDs may inhibit viral infection by regulating the mRNA expression levels of interferon-stimulated genes.

2.7. Gly-CDs Inhibit ROS Production in PRRSV-Infected MARC-145 Cells

Reactive oxygen species (ROS) play an essential role in regulating various physiological diseases, such as brain diseases, inflammatory diseases, cardiovascular diseases, bacterial infection, and so on.[67] Viral infection causes an increase in intracellular ROS, thereby blocking the signaling pathways in the body's natural immunity. Reducing the ROS level by their inhibitors can inhibit virus proliferation. It is reported that the intracellular ROS levels can be successfully regulated to suppress viral infection by embedding poly(aniline-co-pyrrole) within an amphiphilic methoxy polyethylene glycol-block-polyphenylalanine copolymer.[68] Another study has shown that silver nanoparticle-based codelivery of oseltamivir could remarkably inhibit the accumulation of ROS and activate the signaling pathways of AKT and p53 phosphorylation to inhibit H1N1 influenza virus infection.[69] Whether Gly-CDs can regulate the cellular ROS level was investigated in this study. Briefly, after PRRSV infection for 1–2 h, the MARC-145 cells were treated separately with Gly-CDs for 12 h, then an inverted fluorescence microscope was used to detect the cellular ROS levels by detecting the fluorescence of 2',7'-dichlorofluorescein (DCF). In **Figure 7**, green fluorescence indicates the presence of ROS, and the level of PRRSV-induced ROS was significantly reduced in the Gly-CDs treatment versus the PPRSV treatment (Mock).

Such experimental results suggest that Gly-CDs can inhibit viral proliferation by suppressing the production of PRRSV-induced ROS.

2.8. Gly-CDs Regulate the Expression of Antiviral Genes DDX53 and NOS3 in MARC-145 Cells

The antiviral mechanisms of Gly-CDs were further explored at the intracellular protein level by isobaric tag for relative and absolute quantitation (iTRAQ) quantitative proteomic analysis. Briefly, MARC-145 cells were incubated or mock-incubated (DMEM containing 2% serum) with Gly-CDs at 0.30 mg mL^{-1} for 24 h. Subsequently, a series of experiment was carried out according to the experimental flow chart of Scheme S2, Supporting Information, the quality test results of the collected cell samples indicate that the samples meet the quality requirements (Figure S6, Supporting Information). Furthermore, a total of 60 036 peptides and 7364 proteins were identified by searching against the Macaca mulatta Uniprot Proteome database, including 31 proteins that are differentially expressed (total protein data and differentially expressed protein data can be found in the attached excel). A dot-plot was also supplied to present the overview of quantified proteins and differentially expressed cellular proteins (Figure S7, Supporting Information). Among them, seven differentially expressed proteins and two non-differentially expressed proteins were detected by Western blot assay to validate the liquid chromatography tandem-mass spectrometry (LC-MS/MS) data. In **Figure 8**a, it was shown that in Gly-CDs-treated cells, the expressions were downregulated in thioredoxin-like protein 1 (TXNL1), nitric oxide synthase (NOS3), and olfactomedin 4 (OLFM4),
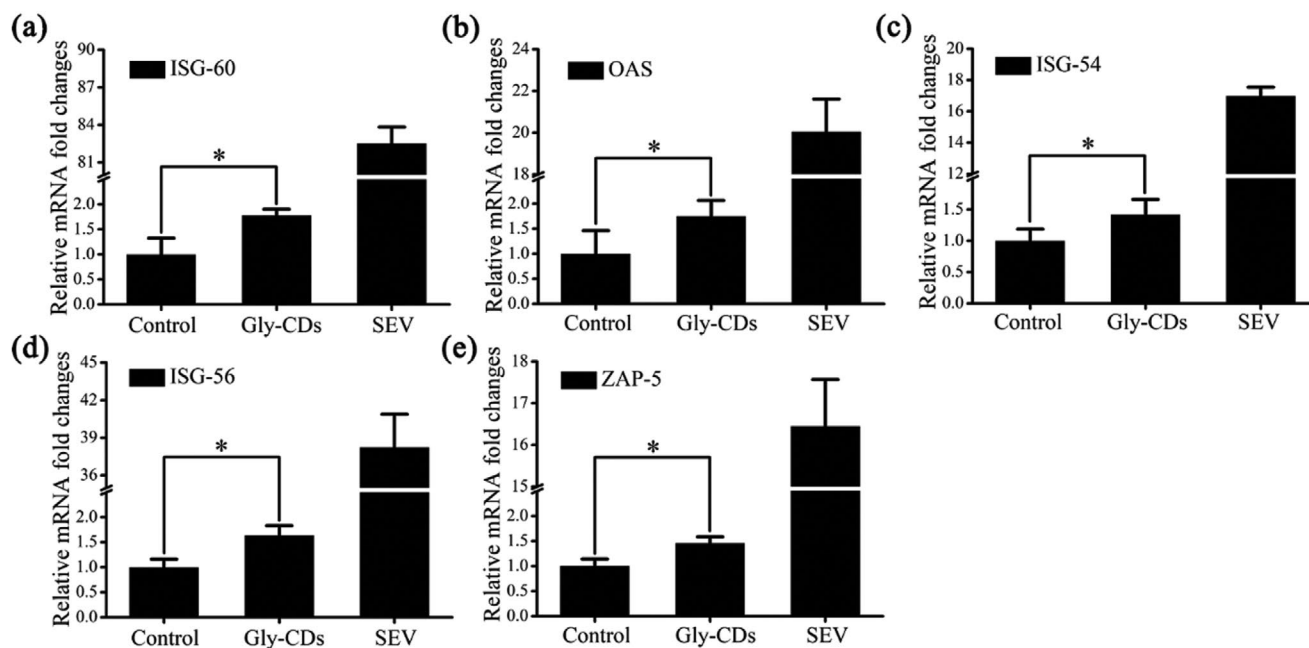

Figure 6. Cytokine expression in MARC-145 cells induced by 0.30 mg mL^{-1} Gly-CDs and Cit-Cds. MARC-145 cDNA samples were used for real-time RT-qPCR analysis of the expressions in a) ISG-60, b) OAS, c) ISG-54, d) ISG-56, and e) ZAP-5. GAPDH was used to normalize the gene expression. Data are shown as the mean values ± SD from three replications.

ADVANCED
SCIENCE NEWS
www.advancedsciencenews.com

NANO · MICRO
small
www.small-journal.com
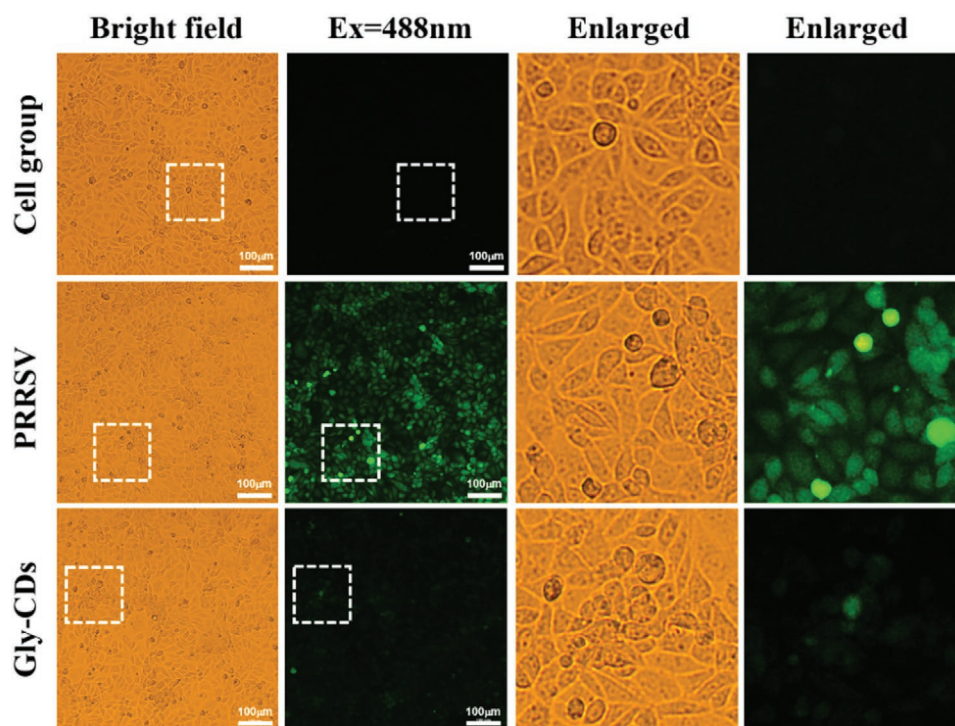
Figure 7. Cellular ROS levels in PRRSV-infected MARC-145 cells post different treatments. The cell group indicated normal cells in the absence of Gly-CDs and PRRSV. The mock group indicated the PRRSV-infected cells without CDs treatment. Gly-CDs group represent the PRRSV-infected cells treated with Gly-CDs. Scale bar = 100 μm.

upregulated in cathepsin D (CTSD), colony stimulating factor 1 (CSF1), and pyridoxal phosphate phosphatase (PDXP), and not significantly changed in 60 kDa heat shock protein (HSPD1), and mitochondrial and vimentin (VIM). The gray value was converted to the quantitative result by ImageJ software and the ratios (Gly-CDs/Control) identified by Western blot assay were consistent with those from iTRAQ-based proteomic analysis.

As previously reported, RNA helicases are involved in nearly all aspects of RNA metabolism, from transcription and translation to mRNA decay, and they are enzymes that use ATP to bind or remodel RNA and RNA-protein complexes, with putative ATP-dependent RNA helicase DDX53 (DDX53) being a member of this family.[70] The knockdown of DDX53 and DDX47 has been reported to increase SFV infection by
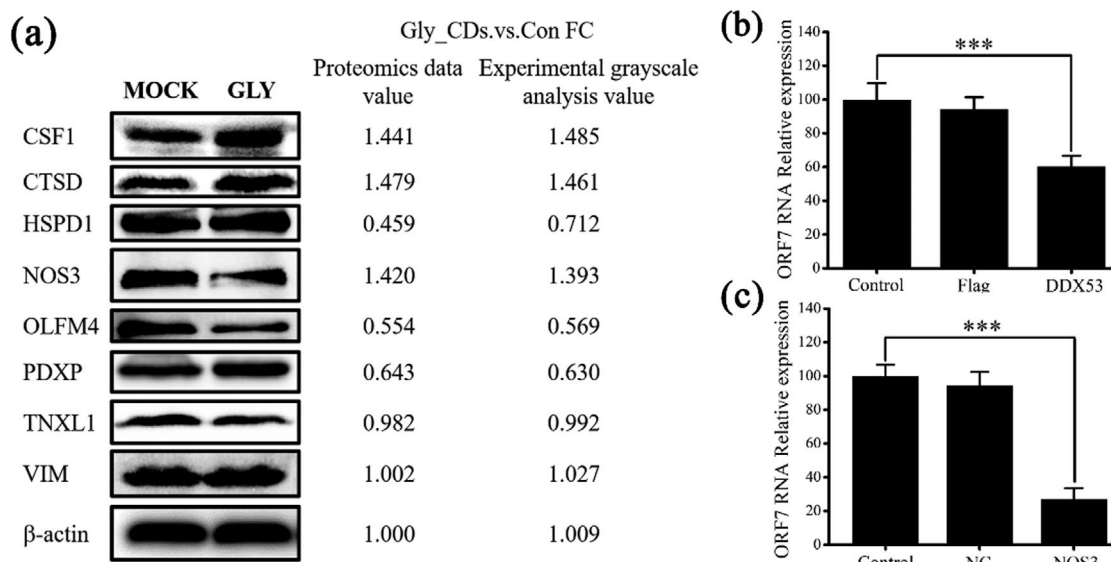
Figure 8. a) Proteomics data from Western blot analysis. RT-qPCR assay of the effect of b) overexpression of DDX53 and c) downregulation of NOS3 on the number of PRRSV ORF7 copies.

affecting the post-penetration stages, but with no effect on VSV infection. DDX60 is a novel antiviral helicase promoting RIG-I-like receptor-mediated signaling.[71] In DDX19-depleted cells, the accumulation of viral RNAs and proteins was delayed, leading to an obvious decrease in the production of infectious influenza A virus particles.[72] In Figure 8b, we can see that the overexpression of DDX53 in MARC-145 cells showed a certain inhibitory effect on the proliferation of PRRSV.

Nitric oxide (NO) regulates the heart by spatial confinement of nitric oxide synthase (NOS) isoforms.[73] NOS3, a dimeric enzyme, is the most important isoform for NO formation in the cardiovascular system, and its expression and activity can be regulated at transcriptional, posttranscriptional, and posttranslational levels.[74] The deficiency of inducible and endothelial NOS was reported to be responsible for delayed union and non-union development as well as diminished bone formation.[75] The cardiomyocyte-restricted overexpression of endothelial NOS3 was shown to attenuate β-adrenergic stimulation and reinforce vagal inhibition of cardiac contraction.[76]

As indicated in Figure 8c, downregulation of NOS3 gene can suppress the proliferation of PRRSV about 30% by RT-qPCR assay. The resulting data of the interferon screening were introduced by western blot analysis in Figure S8, Supporting Information and the data of the plaque assay confirmed the same results as RT-qPCR assay (Figure S9, Supporting Information).

3. Discussion

So far, there is no efficient treatment for PRRSV in the clinic. As reported, the occurrence and spread of the disease cannot be blocked by the current prevention and treatment strategy that is authorized to use inactivated vaccine and attenuated vaccine.[34] Vaccination could cause hosts to be more susceptible to secondary infection by other viruses or bacteria.[32] So the development of anti-PRRSV drugs have imperative academic research value and clinical application prospects.

In recent years, due to their unique properties and biocompatibility, especially non-toxic metabolism, carbon nanomaterials including CDs,[9,10,14,77] nanographene sheets,[43,78] graphene quantum dots,[13] have been extensively investigated and proved to have outstanding antiviral effects. They are prepared by polyglycerol, 4-aminophenylboronic acid hydrochloride, benzoxazine, PEG-diamine, 3-ethoxypropylamine, curcumin, and other raw materials. Studies have shown that the size, charge, and surface modification of carbon nanomaterials have important influence on their antiviral activity. The mechanisms of inhibiting virus were shown to include blocking the entry of virus, improving expression of ISG, changing the structure of surface protein of virus, etc.[9–14,77,78] Virus infection to cells is an extremely complex dynamic process, including changes in the structure of the virus, cellular immune stress, and changes in the microecology of the viral parasitic cells. Therefore, it is necessary to comprehensively explore the mechanism of Gly-CDs action from multiple angles.

In our previous study, we tested the anti-PRRSV activity of glycyrrhizic acid, the results showed that the inhibitory effect of glycyrrhizic acid at 400 μM (0.33 mg mL^{-1}) was ≈2 orders of magnitude.[30] In this study, 0.30 mg mL^{-1} Gly-CDs

inhibited PRRSV proliferation with ≈5 orders of magnitude, indicating that the Gly-CDs increase the antiviral activity of glycyrrhizic acid. In a recent study, Lin et al. reported that the curcumin-carbon quantum dots had higher antiviral effect than curcumin on the proliferation of enterovirus 71, which is in agreement with our results.[77] As shown by the infrared spectra in Figure 1f, Gly-CDs were similar to glycyrrhizic acid in structure, with most functional groups of glycyrrhizic acid being maintained during the formation of Gly-CDs. However, Gly-CDs have large surface area and more contact sites as compared with glycyrrhizic acid, leading to polyvalent interactions with the virus and thus higher antiviral activity than glycyrrhizic acid, similar to the enhanced antiviral activity of gold nanoparticles capped with mercaptoethanesulfonate.[79,80] The TEM images of PRRSV with and without Gly-CDs (Figure S10, Supporting Information) also proved that Gly-CDs could interact with PRRSV directly, which may result in inhibition of PRRSV proliferation. Gly-CDs were found to inhibit PRRSV invasion and replication, which is a more significant physiological process. However, the visual exploration of Gly-CDs in the virus penetration process is difficult and needs to be improved in further studies.

The hydrothermal reaction source, temperature, and time have great effects on the size and functional groups of as-prepared CDs, which could further affect the antiviral activity of CDs.[77] In our study, the control (Cit-CDs) was used mainly to explore the influence of the synthetic materials of CDs on their antiviral activity. The results (Figure 3) showed that Cit-CDs had no significant inhibitory effect on the proliferation of PRRSV, indicating that the source of CDs had an important effect on their antiviral activity. What is more, we compared the anti-PRRSV activity of Gly-CDs prepared under hydrothermal reaction for different time periods (7 h, 14 h) (Figure S11, Supporting Information). The inhibitory effect of 14h-Gly-CDs was shown to be inferior to that of 7h-Gly-CDs, probably due to difference in functional groups of CDs. This suggests the potential relationship of the functional groups on the surface of Gly-CDs with antiviral activity, which needs further study.

We also systematically explored cellular immune stress caused by viral infection, including changes in ROS production and protein expression levels in cells, changes in viral gene levels, protein levels, and infectivity. The induction of ISG expression is a classical broad antiviral pathway for elucidating the antiviral mechanism.[81] Gly-CDs can induce the upregulation of IFN-stimulating genes, which can be the main reason for its potential use as a broad-spectrum antiviral agent, including PEDV and PRV. However, Gly-CDs appear to exhibit stronger antiviral activity against RNA viruses (PRRSV and PEDV in this study) than DNA viruses (PRV in this study). Previous studies demonstrated that CDs can induce the production of IFN and IFN-stimulating genes.[10] However, viruses vary in their susceptibility to interferon, implying the Gly-CDs may also vary in antiviral activity against different viruses. Additionally, we cannot rule out the possibility of other unidentified mechanisms attributed to the broad-spectrum antiviral activity of Gly-CDs.

Mass spectrometry-based proteomics can help us to accurately identify and quantify the proteins involved in cellular events, such as cellular responses to nanoparticles underlying

nano-bio-interactions. Proteomics technology can identify the structural functions and expression levels of specific proteins in sample tissues, understand the pathogenic mechanisms, and alter the expression patterns of different proteins.[82] Thus, iTRAQ proteomic analysis was used to evaluate the differential protein expression in cells after treatment with Gly-CDs as well as the functions of these differential proteins. Based on proteomics data, the action mechanism of Gly-CDs on PRRSV proliferation was explored by some cellular responses from MARC-145 cells induced by Gly-CDs. This means that Gly-CDs can stimulate cells to regulate the expression of some host restriction factors, including DDX53 and NOS3, which have an important role in the subsequent cell infection by PRRSV.

As an active ingredient of the traditional Chinese herbal medicine, glycyrrhizic acid plays an important role in anti-oxidation, anti-inflammation, antiviral immunoregulation, and liver protection.[22–26] However, poor water solubility, relatively high cytotoxicity, and ambiguous action mechanism limit its wide application. Additionally, previous studies have reported the side effects of glycyrrhizic acid, such as hypokalemia, edema, and thrombocytopenia.[83] The Gly-CDs have higher biocompatibility, and theoretically, they can reduce the side effects of glycyrrhizic acid. However, whether the Gly-CDs exhibit stronger antiviral activity in vivo and reduce the side effects of glycyrrhizic acid still needs further study in the host (pig) of PRRSV.

4. Conclusions

In this paper, Gly-CDs were synthesized from the traditional Chinese herbal medicine by hydrothermal method. The chemical characterization demonstrated that Gly-CDs have high dispersibility, small size, and other properties. Biological experiments indicated that Gly-CDs have excellent antiviral activity against PRRSV ($\approx$5 orders of magnitude). The antiviral mechanism of Gly-CDs was demonstrated from inactivation of PRRSV in vitro, inhibition of PRRSV invasion and replication, stimulation of cells to produce interferon, inhibition of ROS production induced by PRRSV infection. Proteomics data also indicated that Gly-CDs can induce upregulation of intracellular antiviral proteins or downregulate pro-viral proteins.

5. Experimental Section

Synthesis of CDs: Glycyrrhizic acid (93%) and Quinine sulfate (99%) were provided by Aladdin Chemistry Co. Ltd. (Shanghai, China). NaOH (AR), ethylenediamine (AR), and citric acid (AR) were obtained from the Sinopharm Chemical Reagent Co. Ltd. (Shanghai, China). All reagents were directly used without further purification. All solutions were prepared with deionized water from a Millipore water purification system. Briefly, the Gly-CDs were synthesized with a modified one-pot hydrothermal method. In a typical synthesis route, 0.10 g (0.12 mmol) glycyrrhizic acid was dissolved in 10 mL deionized water, followed by adding dropwise saturated NaOH aqueous solution to adjust the pH to 10.0 ± 0.2, transferring the mixture into a 25 mL Teflon-lined autoclave and incubation at 180 °C for 7 h (Gly-CDs). After cooling to room temperature naturally, large precipitate was removed from the mixture by centrifugation at 10 000 rpm for 10 min, followed by collecting the supernatant and filtering through a 0.22 μm filter to further remove small precipitate. Finally, the Gly-CDs were obtained by dialysis against

deionized water for 8 h with a cut-off molecular weight 14 kDa dialysis bag, with the deionized water being changed every 2 h during dialysis. The Gly-CDs powders were then collected and freeze-dried for further usage. The quantum yield of the Gly-CDs was measured to be 1.41%, using quinine sulfate as reference.

Cells and Viruses: Porcine kidney (PK-15) cells, African green monkey kidney (Vero) cells, and monkey kidney (MARC-145) cells were purchased separately from the American Type Culture Collection (ATCC) and the China Center for Type Culture Collection (CCTCC). Cells were preserved at 37 °C in 5% CO$_2$ atmosphere as adherent culture in Dulbecco's modified Eagle's medium (DMEM/High glucose, HyClone) mixed with 10% fetal bovine serum (FBS, PAN, USA). When grown to confluence, the cells were washed with PBS and collected from the culture vessel surface by adding 0.06% trypsin.

The HP-PRRSV strain WUH3 (GenBank Accession No. HM853673) (isolated at the end of 2006 in China from the pig brains with the syndrome of "high fever") was transfected into MARC-145 cells as previously reported.[84,85] Meanwhile, PEDV strain AJ1102 (GenBank accession No. JX188454) (isolated in China in 2011 from a sucking piglet suffering from acute diarrhea) was transfected into Vero cells in DMEM containing 10 μg mL^{-1} trypsin.[86] Pseudorabies virus (PRV) strain Ea (GenBank accession No. KX423960) is a wild virulent strain obtained in China. The recombinant PRV expressing GFP (PRV-GFP) was transfected into PK-15 cells.[87]

Cytotoxicity Assay: When grown to 80–90% confluence, MARC-145 cells were seeded in 96-well plates, followed by incubation separately with Gly-CDs, Cit-CDs, or glycyrrhizic acid at different concentrations in DMEM supplemented with 2% FBS for 12, 24, 36, and 48 h. After replacing the supernatant with 100 μL of fresh DMEM (containing 2% FBS), each well was supplemented with 20 μL of MTT (3-[4,5-dimethylthiazol-2-thiazolyl]-2,5-diphenyl tetrazolium bromide, Sigma) solution (5.0 mg mL^{-1}). After incubation for 4 h, the supernatant was removed, and the formazan crystals were dissolved in 150 μL per well of dimethyl sulfoxide (DMSO) solution. After shaking on rocking shaker for 10 min at 150 rpm, the OD values at 570 nm were measured for estimating the percentage of cell relative viability using an enzyme linked immunosorbent assay microplate reader.

Antiviral Assay: Briefly, MARC-145 cells were incubated with CDs at 0.30 mg mL^{-1} in DMEM (containing 2% FBS) for 2 h, and RRRSV was preincubated with CDs at 0.30 mg mL^{-1} for 1 h at 4 °C. Then the medium containing CDs was removed and substituted with the pretreated PRRSV at multiplicity of infection (MOI) of 1. After incubation for 1 h, the supernatant was discarded, and cells were washed twice with DMEM, followed by incubation separately with CDs at 0.30 mg mL^{-1} for 12, 24, 36, and 48 h. The antiviral effect of Gly-CDs on PRRSV infection was then evaluated by plaque assay, IFA, Western blot assay, and RT-qPCR assay. For plaque assay, the supernatant is collected at the indicated time point, then the fresh medium is added to the cells and the cells were stored at −80 °C; after freeze-thawing three times, the sample was collected as a cell lysate. All collected samples were stored in −80 °C and the amount of virus in the samples was quantified by plaque assay.

The antiviral effect of Gly-CDs on PEDV and PRV in Vero cells and PK-15 cells at the concentrations of 0.30 mg mL^{-1} was detected in a similar way as described above. Briefly, PK-15 cells were infected with GFP-PRV (MOI = 1) for the indicated periods of time. Vero cells were infected with PEDV (MOI = 0.1) for the indicated periods of time.

Inactivation Assay: PRRSV was incubated with 0.30 mg mL^{-1} Gly-CDs at 37 °C for 1 h. After pre-cooling at 4 °C for 30 min, MARC-145 cells were infected with the pretreated PRRSV at 4 °C for 2 h, followed by plaque assay.

Adsorption Assay: MARC-145 cells were precooled at 4 °C for 30 min, followed by infection with PRRSV (MOI = 0.001) for 2 h at 4 °C in the presence of 0.30 mg mL^{-1} Gly-CDs in DMEM (containing 2% FBS). After discarding the supernatant, the cells were washed twice with precooled serum-free DMEM for plaque assay.

Invasion Assay: After precooling at 4 °C for 30 min, the MARC-145 cells were infected with PRRSV (MOI = 0.1, 0.0001) at 4 °C for 2 h. After discarding the supernatant and two washes with precooled serum-free

ADVANCED
SCIENCE NEWS
www.advancedsciencenews.com

NANO · MICRO
small
www.small-journal.com

DMEM, the cells were incubated with 0.30 mg mL^{-1} Gly-CDs in DMEM (containing 2% FBS) for 3 h at 37 °C. After two washes with serum-free DMEM, the plaque assay was performed.

Replication Assay: When MARC-145 cells were cultured to 80–90% confluence in 24-well plates, the supernatant was discarded and the cells were infected with PRRSV (MOI = 1) at 37 °C for 1 h. Next, the virus inoculum was discarded and the cells were washed twice with serum-free DMEM to remove non-adsorbed virus particles, followed by culture in DMEM (2% FBS) for another 6 h. Subsequently, the cells were incubated separately with 0.30 mg mL^{-1} Gly-CDs in DMEM (containing 2% FBS) for 7, 8, 9, or 10 h. Finally, the total RNA was isolated and the negative-sense RNA of PRRSV was quantified by RT-qPCR assay.

Release Assay: Briefly, PRRSV (MOI = 1) was added to the 24-well plates covered with monolayer MARC-145 cells. After absorption at 37 °C for 1 h, the non-adsorbed virus particles were removed by two washes with serum-free DMEM, then the cells were cultured in DMEM (containing 2% FBS) for another 18 h. After discarding the supernatant and two washes with serum-free DMEM, the cells were incubated separately with 0.30 mg mL^{-1} Gly-CDs in DMEM (containing 2% FBS). At 15, 30, 45, or 60 min, the supernatant was collected and stored at −80 °C. Meanwhile, fresh medium is added to the cells and the cells were stored at −80 °C; after freeze-thawing three times, the sample was collected as a cell lysate. Finally, the virus content in the supernatant and cell lysis were detected by plaque assay.

Evaluation of ROS Production: The intracellular generation of ROS was evaluated using Reactive Oxygen Species Assay Kit (Beyotime, S0033). Briefly, after PRRSV infection for 1–2 h, the MARC-145 cells were treated separately with Gly-CDs for 12 h, followed by two washes with PBS and staining with 1 mL of 5 μM fluorescence marker 2′,7′-dichlorofluorescein diacetate (DCF-DA) for 30 min in the dark at 37 °C in 5% CO$_2$. After removing the staining solution and washing twice with PBS, an inverted fluorescence microscope was used to evaluate the relative level of ROS production by observing the fluorescence images. For excitation, an argon laser with a wavelength of 488 nm was used and the fluorescent DCF was analyzed at an emission wavelength of 525 nm.

iTRAQ Quantitative Proteomic Analysis: Briefly, cells were cultured to 100% confluence, followed by dividing into two groups: treatment with 0.30 mg mL^{-1} Gly-CDs or DMEM (2% FBS) for 24 h. In each group, there were five biological replicates, with three of them used for iTRAQ quantitative proteomics analysis, and two of them used as parallel experiments to verify the reliability of the proteomics data. For proteomics analysis, the medium was removed at the end of exposure and cells were washed three times with precooled PBS. Next, 10 mL of ice-cold PBS was added and cells were harvested using a cell scraper. Cell suspensions were transferred to 50 mL Falcon tubes, followed by centrifugation at 4000 rpm for 10 min, discarding the supernatant and freezing the cell pellet at the liquid nitrogen tank for further analysis. The other two parallel experimental samples were compiled utilizing the observational method of Western blot assay. For other experimental methods and procedures regarding total protein extraction, protein examination, iTRAQ mark, fraction separation, and data analysis, refer to the Supporting Information.

Supporting Information

Supporting Information is available from the Wiley Online Library or from the author.

Acknowledgements

Conflict of Interest

The authors declare no conflict of interest.

Keywords

[1] S. Y. Lim, W. Shen, Z. Gao, *Chem. Soc. Rev.* **2015**, *44*, 362.
[2] M. L. Liu, B. B. Chen, C. M. Li, C. Z. Huang, *Green Chem.* **2019**, *21*, 449.
[3] H. Yang, Y. Liu, Z. Guo, B. Lei, J. Zhuang, X. Zhang, Z. Liu, C. Hu, *Nat. Commun.* **2019**, *10*, 1789.
[4] B. Yao, H. Huang, Y. Liu, Z. Kang, *Trends Chem.* **2019**, *1*, 235.
[5] P. Huang, J. Lin, X. Wang, Z. Wang, C. Zhang, M. He, K. Wang, F. Chen, Z. Li, G. Shen, D. Cui, X. Chen, *Adv. Mater.* **2012**, *24*, 5104.
[6] L. Pan, S. Sun, A. Zhang, K. Jiang, L. Zhang, C. Dong, Q. Huang, A. Wu, H. Lin, *Adv. Mater.* **2015**, *27*, 7782.
[7] V. Georgakilas, J. A. Perman, J. Tucek, R. Zboril, *Chem. Rev.* **2015**, *115*, 4744.
[8] A. Barras, Q. Pagneux, F. Sane, Q. Wang, R. Boukherroub, D. Hober, S. Szunerits, *ACS Appl. Mater. Interfaces* **2016**, *8*, 9004.
[9] S. Huang, J. Gu, J. Ye, B. Fang, S. Wan, C. Wang, U. Ashraf, Q. Li, X. Wang, L. Shao, Y. Song, X. Zheng, F. Cao, S. Cao, *J. Colloid Interface Sci.* **2019**, *542*, 198.
[10] T. Du, J. Liang, N. Dong, L. Liu, L. Fang, S. Xiao, H. Han, *Carbon* **2016**, *110*, 278.
[11] T. Du, N. Dong, L. Fang, J. Lu, J. Bi, S. Xiao, H. Han, *ACS Appl. Nano Mater.* **2018**, *1*, 1731.
[12] H. Liu, Y. Bai, Y. Zhou, C. Feng, L. Liu, L. Fang, J. Liang, S. Xiao, *RSC Adv.* **2017**, *7*, 28016.
[13] D. Iannazzo, A. Pistone, S. Ferro, L. De Luca, A. M. Monforte, R. Romeo, M. R. Buemi, C. Pannecouque, *Bioconjugate Chem.* **2018**, *29*, 3084.
[14] X. Dong, M. M. Moyer, F. Yang, Y. P. Sun, L. Yang, *Sci. Rep.* **2017**, *7*, 519.
[15] R. K. Ganjhu, P. P. Mudgal, H. Maity, D. Dowarha, S. Devadiga, S. Nag, G. Arunkumar, *VirusDisease* **2015**, *26*, 225.
[16] W. Li, X. H. Wang, Z. Luo, L. F. Liu, C. Yan, C. Y. Yan, G. D. Chen, H. Gao, W. J. Duan, H. Kurihara, Y. F. Li, R. R. He, *Int. J. Mol. Sci.* **2018**, *19*, 3266.
[17] Z. Wang, Y. Zhu, *Health* **2010**, *02*, 1397.
[18] W. Chen, C. E. Lim, H. J. Kang, J. Liu, *PLoS One* **2011**, *6*, e28093.
[19] J. H. Li, R. Q. Wang, W. J. Guo, J. S. Li, *J. Chin. Med. Assoc.* **2016**, *79*, 281.
[20] T. N. Wu, K. C. Yang, C. M. Wang, J. S. Lai, K. N. Ko, P. Y. Chang, S. H. Liou, *Sci. Total Environ.* **1996**, *182*, 193.
[21] A. B. Abt, J. Y. Oh, R. A. Huntington, K. K. Burkhart, *Arch. Intern. Med.* **1995**, *155*, 211.
[22] R. Pompei, O. Flore, M. A. Marccialis, A. Pani, B. Loddo, *Nature* **1979**, *281*, 689.
[23] L. J. Ming, A. C. Yin, *Nat. Prod. Commun.* **2013**, *8*, 415.
[24] K. Akutagawa, T. Fujita, K. Ouhara, T. Takemura, M. Tari, M. Kajiya, S. Matsuda, S. Kuramitsu, H. Mizuno, H. Shiba, H. Kurihara, *Int. Immunopharmacol.* **2019**, *68*, 30.
[25] O. Y. Selyutina, N. E. Polyakov, *Int. J. Pharm.* **2019**, *559*, 271.
[26] Q. Zhang, M. Ye, *J. Chromatogr. A* **2009**, *1216*, 1954.

[27] H. Zhao, Z. Liu, H. Shen, S. Jin, S. Zhang, *Eur. J. Pharmacol.* **2016**, *781*, 92.

[28] X. Sun, X. Duan, C. Wang, Z. Liu, P. Sun, X. Huo, X. Ma, H. Sun, K. Liu, Q. Meng, *Eur. J. Pharmacol.* **2017**, *806*, 75.

[29] X. Huo, S. Yang, X. Sun, X. Meng, Y. Zhao, *Molecules* **2018**, *23*, 1623.

[30] E. Duan, D. Wang, L. Fang, J. Ma, J. Luo, H. Chen, K. Li, S. Xiao, *Antiviral Res.* **2015**, *120*, 122.

[31] F. C. Størmer, R. Reistad, J. Alexander, *Food Chem. Toxicol.* **1993**, *31*, 303.

[32] T. Du, Y. Nan, S. Xiao, Q. Zhao, E. M. Zhou, *Trends Microbiol.* **2017**, *25*, 968.

[33] T. Dokland, *Virus Res.* **2010**, *154*, 86.

[34] J. K. Lunney, Y. Fang, A. Ladinig, N. Chen, Y. Li, B. Rowland, G. J. Renukaradhya, *Annu. Rev. Anim. Biosci.* **2016**, *4*, 129.

[35] W. Ke, L. Fang, H. Jing, R. Tao, T. Wang, Y. Li, S. Long, D. Wang, S. Xiao, *J. Virol.* **2017**, *91*, 00827.

[36] L. Gao, X. K. Guo, L. Wang, Q. Zhang, N. Li, X. X. Chen, Y. Wang, W. H. Feng, *J. Virol.* **2013**, *87*, 8808.

[37] X. K. Guo, Q. Zhang, L. Gao, N. Li, X. X. Chen, W. H. Feng, *J. Virol.* **2013**, *87*, 1159.

[38] X. Shi, Y. Chang, X. Zhang, L. Wang, C. Li, K. Jiang, J. Chen, C. Wang, R. Deng, J. Fan, G. Zhang, *Res. Vet. Sci.* **2015**, *99*, 215.

[39] J. Xie, H. Zhou, J. Cui, Y. Chen, M. Zhang, S. Deng, P. Zhou, S. Su, G. Zhang, *Infect. Genet. Evol.* **2014**, *28*, 64.

[40] G. Li, J. Huang, P. Jiang, Y. Li, W. Jiang, X. Wang, *Virus Genes* **2007**, *35*, 673.

[41] X. Han, S. Fan, D. Patel, Y. J. Zhang, *Antiviral Res.* **2009**, *82*, 59.

[42] T. Du, J. Lu, L. Liu, N. Dong, L. Fang, S. Xiao, H. Han, *ACS Appl. Bio Mater.* **2018**, *1*, 1286.

[43] H. Liu, Y. Wang, H. Duan, A. Zhang, C. Liang, J. Gao, C. Zhang, B. Huang, Q. Li, N. Li, S. Xiao, E. M. Zhou, *Vet. Microbiol.* **2015**, *181*, 252.

[44] M. Zhou, C. Li, C. Lu, X. Zhang, Y. Pan, X. Liu, G. Liu, Z. Zhao, B. Sun, *DNA Cell Biol.* **2016**, *35*, 636.

[45] Q. Zhang, C. Huang, Q. Yang, L. Gao, H. C. Liu, J. Tang, W. H. Feng, *J. Immunol.* **2016**, *196*, 2272.

[46] L. Zheng, X. Li, L. Zhu, W. Li, J. Bi, G. Yang, G. Yin, J. Liu, *BMC Vet. Res.* **2015**, *11*, 199.

[47] L. Gao, W. Zhang, Y. Sun, Q. Yang, J. Ren, J. Liu, H. Wang, W. H. Feng, *PLoS One* **2013**, *8*, e63767.

[48] B. Zhi, M. J. Gallagher, B. P. Frank, T. Y. Lyons, T. A. Qiu, J. Da, A. C. Mensch, R. J. Hamers, Z. Rosenzweig, D. H. Fairbrother, C. L. Haynes, *Carbon* **2018**, *129*, 438.

[49] D. Bouzas-Ramos, J. Cigales Canga, J. C. Mayo, R. M. Sainz, J. Ruiz Encinar, J. M. Costa-Fernandez, *Adv. Funct. Mater.* **2019**, *29*, 1903884.

[50] S. Zhu, Q. Meng, L. Wang, J. Zhang, Y. Song, H. Jin, K. Zhang, H. Sun, H. Wang, B. Yang, *Angew. Chem., Int. Ed.* **2013**, *52*, 3953.

[51] S. Tao, S. Lu, Y. Geng, S. Zhu, S. A. T. Redfern, Y. Song, T. Feng, W. Xu, B. Yang, *Angew. Chem., Int. Ed.* **2018**, *57*, 2393.

[52] Y. Song, C. Zhu, J. Song, H. Li, D. Du, Y. Lin, *ACS Appl. Mater. Interfaces* **2017**, *9*, 7399.

[53] X. Miao, X. Yan, D. Qu, D. Li, F. F. Tao, Z. Sun, *ACS Appl. Mater. Interfaces* **2017**, *9*, 18549.

[54] S. Kalytchuk, K. Poláková, Y. Wang, J. P. Froning, K. Cepe, A. L. Rogach, R. Zbořil, *ACS Nano* **2017**, *11*, 1432.

[55] J. Wang, X. Chen, W. Wang, Y. Zhang, Z. Yang, Y. Jin, H. M. Ge, E. Li, G. Yang, *J. Ethnopharmacol.* **2013**, *147*, 114.

[56] L. Wang, R. Yang, B. Yuan, Y. Liu, C. Liu, *Acta Pharm. Sin. B* **2015**, *5*, 310.

[57] G. Wong, J. Lu, W. Zhang, G. F. Gao, *Emerg. Microbes Infect.* **2019**, *8*, 150.

[58] C. Lee, *Virology J.* **2015**, *12*, 193.

[59] R. Wang, Y. J. Zhang, *Biomed Res. Int.* **2014**, *2014*, 315470.

[60] A. C. Bréhin, I. Casadémont, M. P. Frenkiel, C. Julier, A. Sakuntabhai, P. Desprès, *Virology* **2009**, *384*, 216.

[61] D. J. Lenschow, C. Lai, N. Frias-Staheli, N. V. Giannakopoulos, A. Lutz, T. Wolff, A. Osiak, B. Levine, R. E. Schmidt, A. García-Sastre, D. A. Leib, A. Pekosz, K. P. Knobeloch, I. Horak, H. W. Virgin, *Proc. Natl. Acad. Sci. USA* **2007**, *104*, 1371.

[62] T. Imaizumi, H. Yoshida, R. Hayakari, F. Xing, L. Wang, T. Matsumiya, K. Tanji, S. Kawaguchi, S. Murakami, H. Tanaka, *Neurosci. Res.* **2016**, *105*, 35.

[63] J. W. Schoggins, S. J. Wilson, M. Panis, M. Y. Murphy, C. T. Jones, P. Bieniasz, C. M. Rice, *Nature* **2011**, *472*, 481.

[64] M. R. MacDonald, E. S. Machlin, O. R. Albin, D. E. Levy, *J. Virol.* **2007**, *81*, 13509.

[65] J. Melchjorsen, H. Kristiansen, R. Christiansen, J. Rintahaka, S. Matikainen, S. R. Paludan, R. Hartmann, *J. Interferon Cytokine Res.* **2009**, *29*, 199.

[66] J. Zhu, Y. Zhang, A. Ghosh, R. A. Cuevas, A. Forero, J. Dhar, M. S. Ibsen, J. L. Schmid-Burgk, T. Schmidt, M. K. Ganapathiraju, T. Fujita, R. Hartmann, S. Barik, V. Hornung, C. B. Coyne, S. N. Sarkar, *Immunity* **2014**, *40*, 936.

[67] B. Yang, Y. Chen, J. Shi, *Chem. Rev.* **2019**, *119*, 4881.

[68] H. O. Kim, M. Yeom, J. Kim, A. Kukreja, W. Na, J. Choi, A. Kang, D. Yun, J. W. Lim, D. Song, S. Haam, *Small* **2017**, *13*, 100818.

[69] Y. Li, Z. Lin, M. Zhao, T. Xu, C. Wang, L. Hua, H. Wang, H. Xia, B. Zhu, *ACS Appl. Mater. Interfaces* **2016**, *8*, 24385.

[70] P. Linder, E. Jankowsky, *Nat. Rev. Mol. Cell Biol.* **2011**, *12*, 505.

[71] M. Miyashita, H. Oshiumi, M. Matsumoto, T. Seya, *Mol. Cell. Biol.* **2011**, *31*, 3802.

[72] C. Diot, G. Fournier, M. Dos Santos, J. Magnus, A. Komarova, S. van der Werf, S. Munier, N. Naffakh, *Sci. Rep.* **2016**, *6*, 33763.

[73] L. A. Barouch, R. W. Harrison, M. W. Skaf, G. O. Rosas, T. P. Cappola, Z. A. Kobeissi, I. A. Hobai, C. A. Lemmon, A. L. Burnett, B. O'Rourke, E. R. Rodriguez, P. L. Huang, J. A. Lima, D. E. Berkowitz, J. M. Hare, *Nature* **2002**, *416*, 337.

[74] G. H. Oliveira-Paula, R. Lacchini, J. E. Tanus-Santos, *Gene* **2016**, *575*, 584.

[75] D. M. Meesters, S. Neubert, K. A. P. Wijnands, F. L. Heyer, S. Zeiter, K. Ito, P. R. G. Brink, M. Poeze, *Bone* **2016**, *83*, 111.

[76] P. B. Massion, C. Dessy, F. Desjardins, M. Pelat, X. Havaux, C. Belge, P. Moulin, Y. Guiot, O. Feron, S. Janssens, J. L. Balligand, *Circulation* **2004**, *110*, 2666.

[77] C. J. Lin, L. Chang, H. W. Chu, H. J. Lin, P. C. Chang, R. Y. L. Wang, B. Unnikrishnan, J. Y. Mao, S. Y. Chen, C. C. Huang, *Small* **2019**, *15*, 1902641.

[78] I. S. Donskyi, W. Azab, J. L. Cuellar-Camacho, G. Guday, A. Lippitz, W. E. S. Unger, K. Osterrieder, M. Adeli, R. Haag, *Nanoscale* **2019**, *11*, 15804.

[79] D. Baram-Pinto, S. Shukla, A. Gedanken, R. Sarid, *Small* **2010**, *6*, 1044.

[80] W. Bing, H. Sun, Z. Yan, J. Ren, X. Qu, *Small* **2016**, *12*, 4713.

[81] S. Y. Liu, D. J. Sanchez, R. Aliyari, S. Lu, G. Cheng, *Proc. Natl. Acad. Sci. USA* **2012**, *109*, 4239.

[82] B. Aslam, M. Basit, M. A. Nisar, M. Khurshid, M. H. Rasool, *J. Chromatogr. Sci.* **2017**, *55*, 182.

[83] M. M. Celik, A. Karakus, C. Zeren, M. Demir, H. Bayarogullari, M. Duru, M. Al, *Hum. Exp. Toxicol.* **2012**, *31*, 1295.

[84] W. Liu, L. Fang, S. Li, Q. Li, Z. Zhou, Z. Feng, R. Luo, G. Shao, L. Wang, H. Chen, S. Xiao, *J. Bacteriol.* **2010**, *192*, 5844.

[85] B. Li, L. Fang, X. Guo, J. Gao, T. Song, J. Bi, K. He, H. Chen, S. Xiao, *J. Clin. Microbiol.* **2011**, *49*, 3175.

[86] J. Bi, S. Zeng, S. Xiao, H. Chen, L. Fang, *J. Virol.* **2012**, *86*, 10910.

[87] H. Zhang, L. Fang, Q. Zhao, N. Xue, Y. Jiang, S. Xiao, H. Chen, *Acta Vet. Zootech. Sin.* **2007**, *38*, 369.